

## MAGNETOHYDRODYNAMIC LIGHT SOURCE WITH A HIGH-TEMPERATURE CURRENT SHEET

S. S. Katsnel'son, N. P. Gridnev, and  
G. A. Pozdnyakov

UDC 533.95;537.84

*Mathematical modeling of a magnetohydrodynamic (MHD) light source based on the physical phenomenon of a C sheet has been performed. The disk scheme of an MHD energy converter where the radiator is a high-temperature current sheet resulting from the interaction of the gas flow with the magnetic field has been selected as the light source. The calculations have been carried out within the framework of the unsteady equations of magnetic hydrodynamics for a viscous compressible heat-conducting gas with allowance for radiative heat transfer and turbulence. The process of formation of the current sheet in the presence of the radiative heat exchange and the outgoing radiation has been studied. It has been shown that the radiation from the C sheet is reabsorbed in colder regions of the flow; however this does not lead to the smearing of the current region and no constriction of the current is observed. The integral characteristics of the radiation, including those of the outgoing-radiation flux, have been calculated.*

The light source in question belongs to the category of plasma sources where the radiator is a high-temperature current sheet (C sheet). A feature distinguishing such a source from the already existing sources, for example, from those employing laminar pulsed discharge [1], is the indestructibility of structural elements and hence the possibility of obtaining high power in the pulse-periodic regime over a protracted period determined by the parameters of the generator of a gasdynamic glow.

The physical phenomenon of a C sheet and organization of flows with current-carrying sheets based on it have been the focus of numerous works, for example, [2–6]. It was established that a characteristic feature of the C sheet is localization of the current in a certain mass of the gas; this localization is stably preserved as a result of the dynamic equilibrium between the Joule heating and the energy loss where of prime importance is the radiation loss. The role of the latter in forming the structure of a current-carrying sheet turned out to be the least understood. The investigations of nonuniform flows with a C sheet as applied to the problems of conversion of energy which were performed in a disk MHD channel [4, 7] turned out to be the most advanced experimentally. Also, such a scheme seems optimum from the viewpoint of creation of a light source.

**Formulation of the Problem.** We carry out calculation-theoretical investigations within the framework of the unsteady equations of magnetic hydrodynamics for a compressible heat-conducting gas with allowance for radiative heat transfer and turbulence. It is obvious that such a problem is practically insoluble in the general formulation and we must introduce reasonable simplifying assumptions which can be made if a specific setup is taken as the object of investigation. As such a setup we consider an experimental setup whose schematic diagram is presented in Fig. 1 (a detailed description is given in [7]). By virtue of axial symmetry, we will solve a two-dimensional axisymmetric problem. Based on the measurements of the deformations of the magnetic field, which did not exceed 10%, we can infer that the magnetic Reynolds number is small. In this case we can disregard the induced field and consider conducting-gas flow in the prescribed magnetic field, which will be assumed to be constant and normal to the velocity vector.

The turbulence will be taken into account on the basis of the simplest semiempirical models. We use the Prandtl expression  $\tau_t = \rho l_t^2 |\partial v / \partial y| \partial v / \partial y$  for the turbulent tangential stress. The presence of the magnetic field leads to a suppressed turbulence, which is usually taken into account in semiempirical theories by decreasing the scale of turbulent pulsations. The expression  $l_t = l_0 \exp(-\beta N \partial v / \partial y)$ , where  $N = \sigma B^2 b / (\rho v)$  is the Stewart number, has been proposed in [8] for the pulsation scale. The parameter  $\beta$  is selected from the condition of equality of the coefficients

---

Institute of Theoretical and Applied Mechanics, Siberian Branch of the Russian Academy of Sciences, Novosibirsk, Russia; email: savelii@itam.nsc.ru. Translated from *Inzhenerno-Fizicheskii Zhurnal*, Vol. 76, No. 1, pp. 114–119, January–February, 2003. Original article submitted April 8, 2002; revision submitted June 11, 2002.

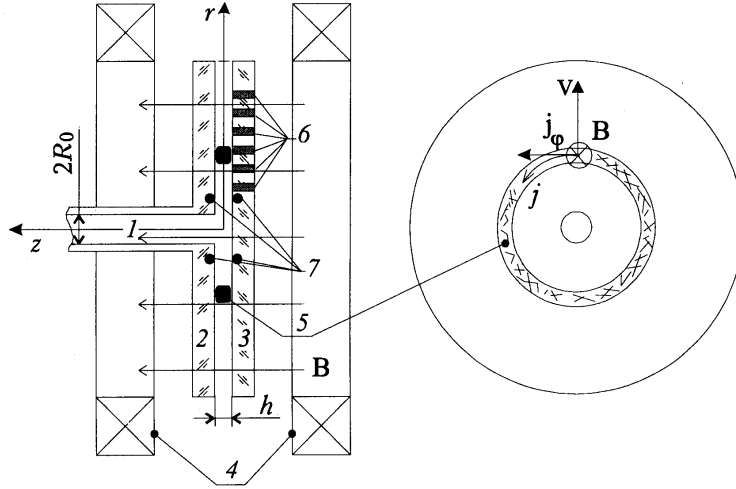


Fig. 1. Conventional diagram of the setup: 1) plasma source; 2) unremovable disk; 3) removable disk; 4) electromagnet coils; 5) C sheet; 6) sensor jacks; 7) coils of the system of initiation of the C sheet.

of resistance of the laminar and turbulent flows for the critical Reynolds number. The known Prandtl–Nikuradze expression [9] is taken as the scale of hydrodynamic turbulence in the channel  $l_0$ . With such an approach we can define the notion of turbulent viscosity ( $\mu_t = \rho l_t^2 |\partial v / \partial y|$ ) and introduce it into the corresponding terms of the system of Navier–Stokes equations in the form of a term to molecular viscosity.

Within the framework of the assumptions made we have  $\mathbf{V}(v_r, 0, v_z)$ ,  $\mathbf{B}(0, 0, B_z)$ ,  $\mathbf{E} = 0$ , and  $\mathbf{j}(0, j_\phi, 0)$ , and the initial system of equations will be written as

$$\frac{\partial F}{\partial t} + \frac{\partial G}{\partial z} + \frac{\partial H}{\partial r} + W = 0, \quad (1)$$

where

$$F = \begin{vmatrix} \rho \\ \rho v_z \\ \rho v_r \\ U \end{vmatrix}, \quad G = \begin{vmatrix} \rho v_z \\ \rho v_z^2 - \sigma_z \\ \rho v_z v_r - \tau_{zr} \\ (U - \sigma_z) v_r - \tau_{zr} v_r - \lambda \frac{\partial T}{\partial z} \end{vmatrix}, \quad H = \begin{vmatrix} \rho v_r \\ \rho v_z v_r - \tau_{zr} \\ \rho v_r^2 - \sigma_r \\ (U - \sigma_r) v_r - \tau_{zr} v_z - \lambda \frac{\partial T}{\partial r} \end{vmatrix},$$

$$W = \frac{1}{r} \begin{vmatrix} \rho v_r \\ \rho v_z v_r - \mu \frac{\partial v_r}{\partial z} - \mu \frac{\partial v_z}{\partial r} + \frac{2}{3} \frac{\partial}{\partial z} (\mu v_r) \\ \rho v_r^2 - 2 \left[ \mu \frac{\partial}{\partial r} \left( \frac{v_r}{r} \right) - \frac{1}{3} \frac{\partial}{\partial r} \left( \frac{\mu v_r}{r} \right) \right] + j_\phi B_z \\ (U + p) v_r + \frac{4}{3} \mu \left[ v_r \frac{\partial v_z}{\partial z} + r v_r \frac{\partial}{\partial r} \left( \frac{v_r}{r} \right) \right] - \lambda \frac{\partial T}{\partial r} \end{vmatrix},$$

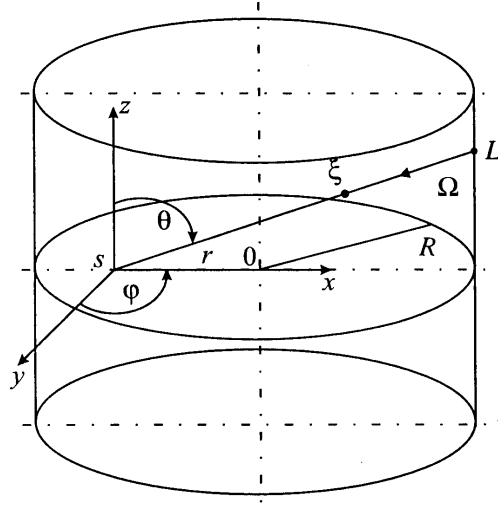


Fig. 2. Toward the calculation of radiation according to the method of partial characteristics.

$$U = \rho \left( c_v T + \frac{1}{2} v_z^2 + \frac{1}{2} v_r^2 \right), \quad \sigma_z = -p - \frac{2}{3} \mu \left( \frac{\partial v_z}{\partial z} + \frac{\partial v_r}{\partial r} \right) + 2\mu \frac{\partial v_z}{\partial z},$$

$$\sigma_r = -p - \frac{2}{3} \mu \left( \frac{\partial v_z}{\partial z} + \frac{\partial v_r}{\partial r} \right) + 2\mu \frac{\partial v_r}{\partial r}, \quad \tau_{zr} = \mu \left( \frac{\partial v_z}{\partial r} + \frac{\partial v_r}{\partial z} \right), \quad j_\varphi = -\sigma_v B_z, \quad \mu = \mu_m + \mu_t.$$

In calculating the transfer of energy by radiation, we employ the following approaches. Where the qualitative picture of formation of flow with a C sheet is investigated, the radiant energy loss is determined based on the limiting approximations by the emissivity factor of hemispherical objects, and the specific power of the radiant loss is represented in the form

$$\nabla \mathbf{S} = \frac{4}{l_{\text{sph}}} \varepsilon_{\text{sph}}(T, p, l_{\text{sph}}) \sigma_C T^4. \quad (2)$$

Such an approach enables us to take correct account of the radiation loss, but it involves an uncontrolled error in determining the temperature profile, especially in the presence of the radiation reabsorption. Nonetheless, the calculations of flows with a C sheet performed earlier within the framework of this approach yielded a good coincidence with the corresponding experimental results [10]. In the cases where a detailed structure of the C sheet is required, the radiation is calculated on the basis of the method of partial characteristics [11]. This method based on the known exact solution of the transfer equation for radiation intensity along the beam  $s \rightarrow L$  (Fig. 2) assumes the replacement of the actual temperature and pressure profiles by a set of model splines for which one computes the optical density  $\tau_v(s) = \int_{\xi}^s k'_v(\xi) d\xi$  in advance and calculates a set of the following integral characteristics required for calculating the flow and

the divergence of the radiation flux:  $\Delta I = \int_0^{\infty} I_{\text{vp}}(T_\xi) k'_v(T_\xi, p_\xi) \exp(-\tau_v(s)) dv$ , which is a functional of the spline ( $\xi \rightarrow s$ ) and takes into account photons that have been generated at the point  $\xi$  and reached the point  $s$  with allowance for the absorption on the path  $\xi \rightarrow s$ :

$$\text{Som} = \int_0^{\infty} I_{\text{vp}}(T_s) k'_v(T_s, p_s) \exp(-\tau_v(s)) dv; \quad \Delta \text{Sim} = \int_0^{\infty} [I_{\text{vp}}(T_\xi) - I_{\text{vp}}(T_s)] k'_v(T_\xi, p_\xi) k'_v(T_s, p_s) dv.$$

For practical calculation of radiative heat exchange the partial characteristics of radiation calculated in advance for a set of basic temperatures, pressures, and beam lengths are selected from [11] for specific gases. The intensity at the point  $s$  of the system in the direction of  $\Omega$  (Fig. 2) is calculated through computation of the integral  $I(s, \Omega) =$

$\int_s^L I(T_\xi, p_\xi, T_s, p_s, l) d\xi$ , where  $T_\xi$  and  $p_\xi$  are the temperature and the pressure at the point  $\xi$  (they are the parameters of the source),  $T_s$  and  $p_s$  are the temperature and the pressure at the calculated point  $s$ , and  $l$  is the length of the segment  $\xi \rightarrow s$ . The field of fluxes is calculated from the formula  $\mathbf{S}(s) = \int_{(4\pi)} I(s, \Omega) \Omega d\Omega$ . To determine the divergence of radiation fluxes we must calculate the quantity  $\nabla I(s, \Omega) = \text{Som}(s, L) - \int_s^L \Delta \text{Sim}(T_\xi, p_\xi, T_s, p_s, l) d\xi$  at the point  $s$  in advance. The effective source of photons  $\text{Som}(s, L)$  which left the point  $s$  in the direction opposite to  $\Omega$ , with allowance for the photon absorption on the path  $s \rightarrow L$ , is determined from  $\Delta I$  according to the rule  $\text{Som}(s, L) = \Delta I(T_s, p_s, T_L, p_L, l)$ , where  $T_s$  and  $p_s$  are the source parameters,  $T_L$  and  $p_L$  are the temperature and the pressure at the boundary of the radiating volume, and  $l$  is the length of the segment  $s \rightarrow L$ . The values of  $\Delta I$ ,  $\text{Som}$ , and  $\Delta \text{Sim}$  in their arguments are determined by interpolating the tabulated values from [11]. Upon calculation of the quantity  $\nabla I$ , we find the divergence of the radiation flux  $\nabla \mathbf{S}(s) = \int_{(4\pi)} \nabla I(s, \Omega) d\Omega$ . In the co-moving spherical coordinate system, the components of the vector  $\mathbf{S}$  and  $\nabla \mathbf{S}$  have the form

$$S_x(s) = \int_0^\pi d\theta \int_0^{2\pi} d\varphi I(s, \theta, \varphi) \sin^2 \theta \cos \varphi, \quad (3)$$

$$S_y(s) = \int_0^\pi d\theta \int_0^{2\pi} d\varphi I(s, \theta, \varphi) \sin^2 \theta \sin \varphi, \quad (4)$$

$$S_z(s) = \int_0^\pi d\theta \int_0^{2\pi} d\varphi I(s, \theta, \varphi) \sin \theta \cos \theta, \quad (5)$$

$$\nabla \mathbf{S}(s) = \int_0^\pi d\theta \int_0^{2\pi} d\varphi \nabla I(s, \theta, \varphi) \sin \theta. \quad (6)$$

The thermophysical and transfer properties of specific working media required for calculations are either prescribed in tabulated form (database) or calculated directly in the program on the basis of the known approximate expressions [10].

Further simplifications in the formulation of the problem are related to the modeling of flow in the experimental setup on the inlet portion of the disk channels where the lock of a shock-heated gas comes out of the straight tube into the disk channel and the flow turns in the radial direction in the system of diffracted and reflected shock waves. The analysis of the results obtained on this setup has shown that when there is no magnetic field in the disk channel a quasi-one-dimensional flow with a characteristic dropping profile of pressure is established behind the shock wave at the periphery of the flow; the pressure profile grows further toward the inlet cross section because of the arrival of the additional mass of the gas in the axial part of the disk channel. Such a situation can be modeled by prescription of a cylindrical shock wave with a certain intensity at the inlet of the disk channel at the initial instant of time followed by the switching-on of a source there which ensures the formation of the required pressure profile.

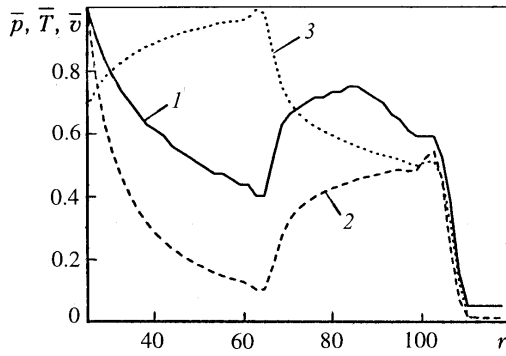


Fig. 3. Results of calculation of the initial flow: 1)  $\bar{p}$ ; 2)  $\bar{T}$ ; 3)  $\bar{v}$ .

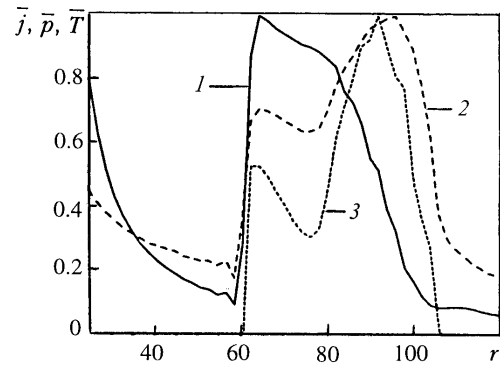


Fig. 4. Results of the calculation in the approximation of volume radiation: 1)  $\bar{p}$ ; 2)  $\bar{T}$ ; 3)  $\bar{j}$ .

To implement the numerical solution of the system of equations (1) we employed a difference scheme of third order of accuracy which showed a good performance in problems of such a type [4].

**Calculation Results.** We considered argon as the working gas. The geometric dimensions of the setup were  $h = 20$  mm,  $R_0 = 25$  mm, and  $R = 120$  mm. At the initial instant of time, we prescribed a shock wave with  $M = 8$  at the inlet cross section and thereafter maintained there the corresponding parameters of the flow behind the initial shock wave. The temperature and pressure of the gas ahead of the shock wave were respectively 300 K and 0.03 bar. The magnetic field was prescribed equal to 1.4 T.

Figure 3 gives results of the calculation of the initial flow without a magnetic field at the instant of time  $t = 58$   $\mu$ sec; the flow is one-dimensional in the absence of viscosity and radiation. The distributions of the pressure  $\bar{p}$ , the temperature  $\bar{T}$ , and the velocity  $\bar{v}$  normalized to the maximum values are shown. The dependences obtained numerically reflect all the fundamental features of the corresponding flow in the experimental setup.

The results of investigations into the organization of MHD flows with a C sheet [4, 10] have shown that spontaneous formation of the C sheet is possible in the flow if the parameters of the flow ensure its intense interaction with the magnetic field. Otherwise, the C sheet must be initiated by creating a local zone of higher-than-average conductivity in the flow. For this purpose, in the experimental setup there is a system of initiation (Fig. 1) consisting of symmetrically arranged coils into which a capacitor bank discharges. Since the time of discharge is much shorter than the characteristic time of gas flow in the disk channel, the process of initiation can be modeled in calculations by prescription of the isochoric disturbance of the temperature in a narrow zone (of the order of the channel width) on the initial portion of the disk channel. The temperature in this zone must ensure the level of conductivity necessary for "catching" the disturbance and it is determined by a specific working substance (for argon the temperature is  $\sim 6500$  K). All the results presented below have been obtained for the regimes of initiation of the C sheet in the initial flow. The initial disturbance was prescribed on the interval  $35 \leq r \leq 45$  mm.

With the aim of elucidating the features of formation of a nonuniform flow with a high-temperature current sheet, we calculated flow of a nonviscous heat-conducting gas with allowance for the radiation loss determined in the approximation of volume luminescence. The procedure of finding them was as follows. For each calculation cell (within which the temperature may be considered to be constant) we compute the radiant-energy flux from a hemispherical volume relying on this cell and thereafter determine the sought power of the radiant loss from formula (2). The emissivity factors corresponding to opaque spectral portions must be eliminated from the total value of  $\epsilon_{\text{sph}}$ . The data on  $\epsilon_{\text{sph}}(T, p, l_{\text{sph}})$  for argon are taken from [12]. We note that the flow also remains one-dimensional in this approximation. As the calculations have shown, at the initial stage of initiation we have the decay of the region of higher-than-average pressure in the disturbance zone followed by the formation of two shock waves propagating upstream and downstream. At the subsequent instants of time, because of the interaction of the formed conducting region with the magnetic field, we observe there a temperature growth and finally the formation of a high-temperature current sheet. As a result of the retardation of the C sheet in the magnetic field a wave reflected from it is formed; this wave, moving upstream, merges with the shock wave resulting from the disturbance decay and subsequently this region is

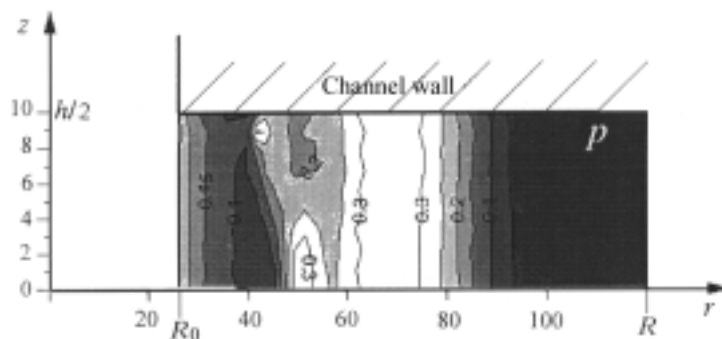


Fig. 5. Pressure field in the disk channel at the instant of time  $t = 85 \mu\text{sec}$ .  $p$ , MPa.

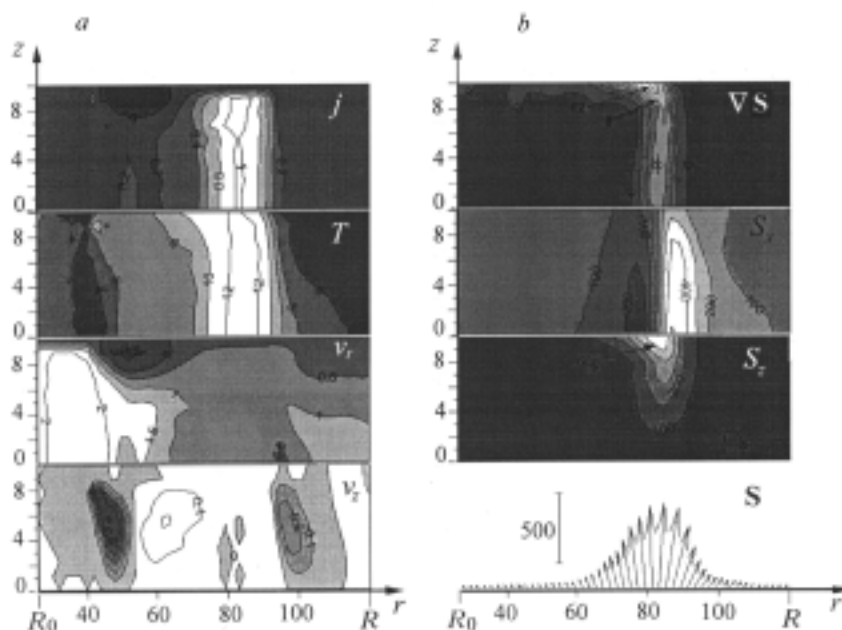


Fig. 6. Distributions of the fields of the gasdynamic parameters of the flow and the current density (a); the divergence of the radiation flux and the components of the vector of radiation flux in the channel and the distribution of the radiation flux along the radius on the disk channel surface (b).  $j$ ,  $\text{kA}/\text{cm}^2$ ;  $T \cdot 10^{-3}$ , K;  $v$ ,  $\text{km}/\text{sec}$ ;  $S$ ,  $\text{kW}/\text{cm}^2$ ;  $r$ , mm.

removed by the flow to the outlet cross section of the channel. Figure 4 gives results of the calculations of the current density, the pressure, and the temperature in the flow at the instant of time  $t = 85 \mu\text{sec}$  when the C sheet has reached the outlet of the channel. The shock wave off the C sheet upstream to which the peak pressure is related is pronounced, whereas the maximum of the temperature coincides with the maximum of the current density in the C sheet. Such a situation is typical of the formation of a nonuniform flow with a C sheet.

Taking account of the viscosity and the radiant heat exchange leads to a spatial pattern of flow. In this case the radiation was calculated based on the method of partial characteristics. The radiant flux and its components and divergence were determined at each point from formulas (3)–(6) using the co-moving coordinate system. The calculation of the radiation also involved the region of the channel  $0 \leq r \leq R_0$ , in which we prescribed an immobile gas with the parameters of the source on  $R_0$ . Test calculations carried out with allowance for just the molecular viscosity on the grid with a small step in the coordinate  $z$  have shown that a very thin boundary layer is formed on the disk surface and the two-dimensional pattern of flow is mainly determined by reabsorbed radiation. Figures 5 and 6a give the distributions of the fields of the gasdynamic parameters of the flow and the current density at the same instant of time  $t$

= 85  $\mu$ sec with allowance for turbulent viscosity. Figure 6b gives results of the calculations of the divergence of the radiation flux and the components of the vector of the radiation flux  $S_x$  and  $S_z$ . The quantity  $S_y$  turned out to be four orders of magnitude lower than  $S_x$  and  $S_z$ , and we can disregard its contribution to the radiant flux. From a comparison of these regimes (Figs. 4–6a) we can infer that in the latter case the velocity of motion of the C sheet (determined, for example, from the maximum of the current density) decreased somewhat. Immediately behind the C sheet upstream, a vortex is formed in the wall region; the temperature in the vortex is higher than that in the ambient gas because of the convective heat transfer. An analysis of the divergence of the radiation flux shows that it is only the region of a strongly heated gas in the C sheet that radiates; in the entire remaining region of the flux, the reabsorption of radiation occurs (in Fig 6b, these are darker regions lying beyond the isolines with a zero mark). The gas adjacent immediately to the current sheet absorbs to a greater extent; however the fraction of absorbed radiation does not exceed 10% of the radiation emitted by the C sheet and this does not lead to a marked smearing of the current region and a regime of the type of a light-detonation wave (the possibility of whose occurrence has been discussed by some researchers) does not occur. The calculations carried out enabled us to answer one of the most important questions as far as the technical applications of a C sheet are concerned: the degree of filling of the channel cross section with the current and the possibility of constricting it. They have demonstrated that the current sheet fills the entire cross section of the channel and continues to be a compact formation in the direction of motion from the instant of its occurrence to the exit from the channel. Figure 6b gives the instantaneous distribution of the radiation flux as viewed from the disk surface of the channel. Noteworthy is a sharp directivity diagram of radiation related directly to the C sheet; the maximum value of the flux at this instant of time is  $\approx 600$  kW/cm<sup>2</sup>. We emphasize that in the C sheet formed the temperature remains constant (at a level of 12,000 K), which ensures the constancy of the outgoing radiation flux.

In closing, it should be said that the results obtained enable us to draw the conclusion on the prospects for employing the above scheme of an MHD energy converter in developments of high-power light sources.

This work was carried out with support from the Russian Foundation for Basic Research, grant No. 99-02-16696.

## NOTATION

$t$ , time;  $r, z, \varphi$ , cylindrical coordinates;  $r, \theta, \varphi$ , spherical coordinates;  $x, y, z$ , Cartesian coordinates;  $\mathbf{V}, \mathbf{B}, \mathbf{E}, \mathbf{j}$ , and  $\mathbf{S}$ , vectors of velocity, magnetic-field induction, electric-field strength, electric-current density, and radiation flux respectively;  $B$ , modulus of the vector of magnetic-field induction;  $v_r$  and  $v_z$ , components of the velocity vector;  $B_z$ , component of the vector of magnetic-field induction;  $j_\varphi$ , component of the current-density vector;  $S_x, S_y$ , and  $S_z$ , components of the radiation-flux vector;  $\tau_t$ , turbulent tangential stress;  $T$ , temperature;  $p$ , pressure;  $\rho$ , density;  $v$ , velocity;  $l_t$ , scale of turbulent pulsations in the plasma in the presence of the magnetic field;  $l_0$ , normal-turbulence scale;  $\sigma$ , conductivity;  $b$ , characteristic dimension of the current region;  $\beta$ , constant;  $\mu_m$ , molecular viscosity;  $\mu_t$ , turbulent viscosity;  $\mu$ , total viscosity;  $\lambda$ , thermal-conductivity coefficient;  $c_v$ , specific heat per unit mass at constant volume;  $\epsilon_{\text{sph}}$ , emissivity factor of the hemispherical volume;  $l_{\text{sph}}$ , radius of the hemispherical volume;  $l$ , segment length;  $\sigma_S$ , Stefan–Boltzmann constant;  $s$ , starting point of the beam;  $L$ , point of intersection of the beam and the surface;  $\nu$ , spectral frequency;  $\tau_\nu$ , spectral optical density;  $k'_\nu$ , spectral coefficient of absorption with allowance for reradiation;  $I_{\text{vp}}$ , spectral intensity of equilibrium radiation;  $\Delta I$ , partial intensity;  $\text{Som}$ , partial source;  $\text{Sim}$ , partial sink;  $I(s, \Omega)$  radiation intensity;  $\Omega$ , unit vector in the direction of quantum motion;  $h$ , channel width;  $R_0$ , radius of the inlet cross section;  $R$ , radius of the outlet cross section;  $M$ , Mach number;  $\bar{p}, \bar{T}, \bar{v}$ , and  $\bar{j}$ , pressure, temperature, velocity, and density of the current normalized to the maximum values. Subscripts: t, turbulent; m, molecular; sph, sphere; 0, zero; v, volume; S, Stefan;  $\nu$ , spectral; vp, spectral equilibrium;  $x, y, z$ , Cartesian coordinates;  $r, \varphi, z$ , cylindrical coordinates;  $\xi, s, L$ , coordinates of the points of definition of the function.

## REFERENCES

1. I. V. Dvornikov, Yu. A. Kolpakov, V. A. Lakutin, and I. V. Podmoshenskii, *Zh. Prikl. Spektrosk.*, **21**, Issue 2, 227–234 (1974).
2. A. N. Tikhonov, A. A. Samarskii, L. A. Zaklyaz'minskii, et al., *Dokl. Akad. Nauk SSSR*, **173**, No. 4, 808–817 (1967).

3. A. I. Zakharov, V. V. Klavdiev, V. D. Pis'mennyi, et al., *Dokl. Akad. Nauk SSSR*, **212**, No. 5, 1092–1095 (1973).
4. N. P. Gridnev, S. S. Katsnel'son, and V. P. Fomichev, *Nonuniform MHD Flows with a C Sheet* [in Russian], Novosibirsk (1984).
5. S. Katsnel'son (Katsnelson), *Progr. Astronaut. Aeronaut.*, **22**, 899–916 (1999).
6. V. A. Ivanov, V. A. Bityurin, A. Vifkind, et al., *Teplofiz. Vys. Temp.*, **31**, 988–994 (1993).
7. G. A. Pozdnyakov, *Experimental Study of a C Sheet in the Model of a Disk MHD Generator on Argon and Sodium Vapor*, Candidate's Dissertation (in Physics and Mathematics), Novosibirsk (1997).
8. G. G. Branover, *Turbulent MHD Flows in Tubes* [in Russian], Riga (1967).
9. H. Schlichting, *Boundary-Layer Theory* [Russian translation], Moscow (1969).
10. S. S. Katsnel'son, *Study of High-Temperature Magnetohydrodynamic Flows in Problems of Energy Conversion*, Doctoral Dissertation (in Physics and Mathematics), Novosibirsk (1997).
11. I. F. Golovnev, V. P. Zamuraev, S. S. Katsnel'son, et al., *Radiative Heat Transfer in High-Temperature Gases* [in Russian], Moscow (1984).
12. S. S. Katsnel'son and G. A. Koval'skaya, *Thermophysical and Optical Properties of an Argon Plasma* [in Russian], Novosibirsk (1985).